Available online at www.sciencedirect.com

ScienceDirect

Procedia Engineering 199 (2017) 3003–3008

Procedia Engineering

www.elsevier.com/locate/procedia

X International Conference on Structural Dynamics, EURODYN 2017

Nonlinear FE model updating of seismic isolated bridge instrumented during the 2010 Mw 8.8 Maule-Chile Earthquake

Yong Li[a]*, Rodrigo Astroza[b], Joel P. Conte[c], Pedro Soto[d]

[a]*Department of Civil & Environmental Engineering, University of Alberta, Edmonton T6G 1H9, Canada*
[b]*Facultad de Ingeniería y Ciencias Aplicadas, Universidad de los Andes, Santiago 7620001, Chile*
[c]*Department of Structural Engineering, University of California, San Diego, La Jolla 92093, the United States*
[d]*Departamento de Ingeniería Civil, Universidad de Chile, Santiago 8330015, Chile*

Abstract

In this paper, nonlinear finite element model updating (FEMU) is performed to study the prediction accuracy of a state-of-the-art finite element (FE) model of a seismic isolated bridge (SIB). The seismic isolator model parameters are updated in two phases: using component-wise and system-wise FEMU. The isolator model parameter values estimated from 23 isolator component tests show a large scatter, and a poor goodness-of-fit (GOF) of the bridge response to the 2010 Maule Earthquake is obtained when most of those parameter sets are used for the isolator elements of the bridge FE model. In contrast, good agreement between the FE predicted and measured bridge response is obtained when the isolator model parameters are calibrated using the bridge response data recorded during the 2010 Mw 8.8 Maule, Chile Earthquake. The updated FE model is then used to reconstruct response quantities not recorded to gain more insight into the effects of seismic isolation during a strong earthquake.

Peer-review under responsibility of the organizing committee of EURODYN 2017.

Keywords: Seismic isolation; Nonlinear finite element model updating; Bridge; 2010 Maule-Chile Megathrust Earthquake; Optimization; Parameter Estimation.

1. Introduction

Highway bridges play a key role in the transportation networks and have been recognized as among the most vulnerable structures to natural disasters, especially to earthquakes [1]. Therefore, the seismic behaviour of highway bridges has been a subject of concern in earthquake-prone countries. Among various low-damage and damage-free

* Corresponding author. Tel.: +1-780-492-2722.
E-mail address: yong9@ualberta.ca

1877-7058
Peer-review under responsibility of the organizing committee of EURODYN 2017.
10.1016/j.proeng.2017.09.397

resilient design strategies (e.g., seismic isolation, self-centering systems), seismic isolation has become an attractive and popular technology to mitigate the damaging effects of earthquakes on bridges and, therefore, enhance their seismic performance [2-3]. The excellent performance of isolated bridges during recent earthquakes has demonstrated the effectiveness of seismic isolation. However, limited investigation of seismic isolated bridge (SIB) structures has been performed using data recorded in situ during strong earthquakes, mainly because of the scarcity of this type of data. Comprehensive comparative studies using data recorded both from laboratory component tests (i.e., component-level tests) and from instrumented SIB structures during earthquakes are even more limited.

Nonlinear finite element (FE) modeling has now become an important tool in design, condition assessment, and performance assessment of civil structures under various loads. Although significant advances have been made in the field of computational structural mechanics (e.g., inelastic constitutive models), the accuracy of nonlinear FE models of large and complex real-world civil structures subjected to strong earthquake excitation needs to be investigated further. A nonlinear FE model of a structure needs to be calibrated in order to minimize the discrepancy between the FE-predicted and measured responses of the structure. This process is known as nonlinear FE model updating (FEMU). In this paper, with a focus on the isolator model parameters, a nonlinear FE model of the bridge developed in the FE analysis software framework *OpenSees* [4] is updated using both the experimental data from component tests on prototypes of the high-damping rubber bearings (HDRBs) of the bridge and the acceleration response data recorded on the Marga-Marga Bridge during the 2010 Mw 8.8 Maule, Chile Earthquake.

2. Description of the Bridge Design, Instrumentation, and FE Modeling

Figure 1 shows the plan and elevation views of the instrumented Marga-Marga Bridge. The bridge superstructure is composed of a RC deck with constant cross section (0.27 m thick by 18.0 m wide) supported by four continuous I girders made of ASTM A-242-81 steel. Five intermediate piers, P#2 to P#6, are supported on pile-group foundations, while the other two piers, P#1 and P#7, and both abutments are supported on shallow foundations. The pier columns are of different heights, and have a double-cell RC box section with dimensions of 2.0 m wide by 10.0 m deep. On the cap beam of each of the seven piers and on the stem wall of each of the two abutments, a group of four bearings are installed to connect the four steel girders with the pier columns and abutments, respectively. The section size of the HDRBs located at the South abutment (SA), pier columns, and North abutment (NA), is $0.50\text{ m} \leftrightarrow 0.50\text{ m}$, $0.85\text{ m} \leftrightarrow 0.55\text{ m}$, and $0.70\text{ m} \leftrightarrow 0.50\text{ m}$, respectively. At the bridge ends, the superstructure is restrained in the transverse direction by stoppers that allow free movement in the longitudinal direction.

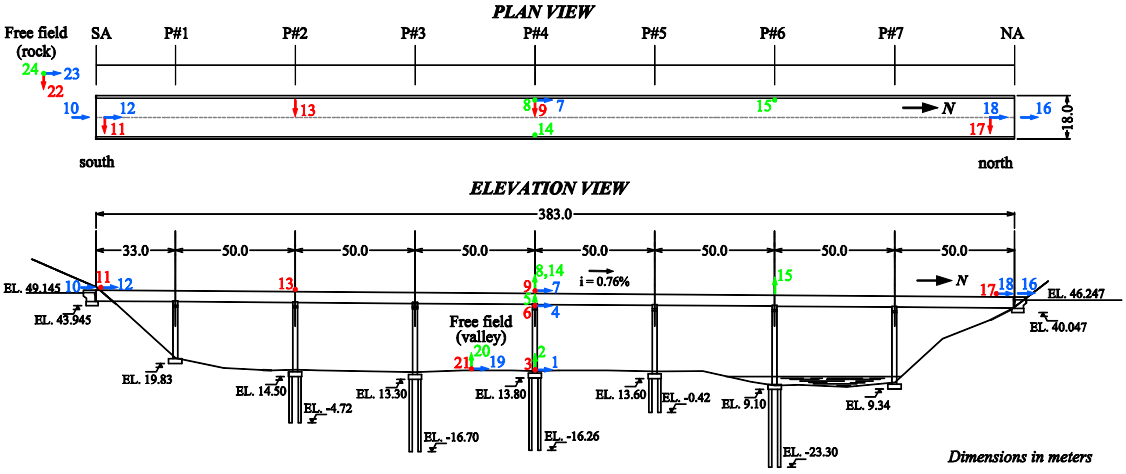

Fig. 1. Plan and elevation views of the instrumented Marga-Marga Bridge, located in the city of Viña del Mar, Chile.

In order to record the base excitation and dynamic response of the bridge, and to investigate the bridge behavior during earthquakes, a total of 24 channels of instrumentation are installed, consisting of nine uniaxial accelerometers and five tri-axial accelerometers [5]. Six uniaxial accelerometers (channels 19 to 21 installed in the valley and channels 22 to 24 close to the South abutment of the bridge) are installed in free-field conditions, while all the other

accelerometers are installed on the bridge structure, i.e., at the bottom and top of bridge pier P#4, on the bridge deck over piers P#2, P#4, and P#6, at both bridge ends, and at both abutments, as shown in Figure 1.

A detailed three-dimensional (3-D) nonlinear FE model of the Marga-Marga Bridge is developed in *OpenSees* (see Figure 2a for a single span view). The bridge superstructure was designed as a capacity protected component to behave quasi linear-elastically, with the four steel girders and the RC deck behaving monolithically. Thus they are modeled using eighteen linear elastic beam-column elements per span. Each bridge pier column is modeled using five or six (depending on the height) displacement-based nonlinear fiber-section beam-column elements. Each of the concrete and steel fibers of each pier is assigned with realistic uni-axial material constitutive models, i.e., using the uniaxial Kent-Park model for concrete fibers and the Giuffre-Menegotto-Pinto model with isotropic strain hardening for steel fibers [4]. Note that a suite of rigid beams, modeled by linear elastic beam-column elements with exceedingly stiff (quasi-rigid) properties, is used to represent geometric offsets. The HDRB isolators are modeled using an elastomeric bearing element with its lateral force-deformation behavior shown in Figure 2b.

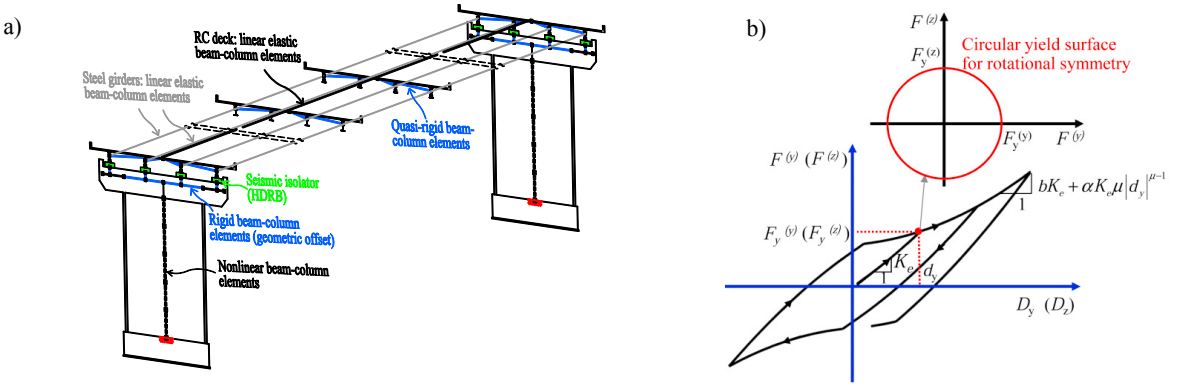

Fig. 2. Schematic view of the 3-D FE modeling: (a) a single span, and (b) lateral force-deformation behavior of the seismic isolator model.

The inertial properties of the bridge structure are calculated based on the mass density and the volume of structural components, and are lumped at the nodes of the FE model. The Rayleigh damping model with a critical damping ratio of 2% assigned at the first transverse and longitudinal modes of the bridge is employed to represent the sources of energy dissipation beyond the energy dissipated through inelastic actions of the materials and seismic isolators. To avoid the introduction of artificial viscous damping in the isolation system, the bearing elements are specified to not contribute to the Rayleigh damping model defined for the overall bridge structure.

The FE model of the bridge considered in this paper does not explicitly model the abutments because the recorded motions at the bridge ends (channels 11, 12, 17, and 18) are imposed as part of the seismic input. Furthermore, the ground motion recorded at the base of pier P#4 (channels 1, 2, and 3) is assumed as the input excitation at the base of all piers. The vertical base excitation is assumed to be uniform over the entire bridge system, i.e., the vertical acceleration recorded at the base of pier P#4 (channel 2) is also used as the vertical excitation at the bridge ends.

3. Nonlinear FE Model Updating of the Bridge Model and Reconstruction of Seismic Response

In this paper, nonlinear FEMU is to minimize the discrepancy between the recorded and FE-predicted response time histories of the bridge, which is measured through a goodness-of-fit metric, i.e., the relative root-mean-square error (RRMSE) of the difference between the time series $r_k^{i,\,recorded}$ and $r_k^{i,\,predicted}$.

$$RRMSE\left(r^i\right)[\%]=\sqrt{\left[1/N_t\sum_{k=1}^{N_t}\left(r_k^{i,\,recorded}-r_k^{i,\,predicted}\right)^2\right]}\Big/\sqrt{\left[1/N_t\sum_{k=1}^{N_t}\left(r_k^{i,\,recorded}\right)^2\right]}\times 100 \quad (1)$$

Here, r denotes the type of response of interest (e.g., displacement), i indicates a specific response record (e.g., response measured at a channel), k designates the time step or discrete time t_k, and N_t is the total number of data

samples considered within a time window (e.g., 40–100 sec).

3.1. Estimation of isolator model parameters using component test data

The experimental data from 23 tests [5] conducted under different loading protocols on prototypes of the 0.85 m ↔0.55 m isolator are used to estimate the model parameters of seismic isolators on top of the bridge piers. A simplified version of the elastomeric bearing model with linear hardening only is used here (i.e., $\alpha = 0$ and $\mu = 1.0$), because it is found to be appropriate to simulate the behavior of the seismic isolators with little nonlinear hardening effect, e.g., during the component tests (maximum lateral deformation of 216 mm) for the isolator prototypes. The calibration of the seismic isolator model using component test data is performed by minimizing the mean-square error between the component test and the numerical model of the isolator test, using a gradient-based optimization tool (*OpenSees-SNOPT*) and a non-gradient-based brute-force optimization approach. Two different starting points for $\boldsymbol{\theta}^0 = [F_y, K_e, b]$ (i.e., $\boldsymbol{\theta}_1^0 = [45.0\,\text{kN}, 10.5\,\text{kN/mm}, 0.19]$, $\boldsymbol{\theta}_2^0 = [30.0\,\text{kN}, 2.8\,\text{kN/mm}, 0.50]$) are considered in *OpenSees-SNOPT*, leading to local minima, $\boldsymbol{\theta}_1^*$ and $\boldsymbol{\theta}_2^*$ respectively. Based on the optimal parameter sets obtained using *OpenSees-SNOPT*, a parameter search space defined by $F_y \in [5.0, 100.0]\,kN$, $K_e \in [5.55, 30.55]\,kN/mm$, $b \in [0.15, 0.80]$, and sampled on a 12↔12↔10 uniform mesh is employed for the grid-based optimization approach to obtain the global minima $\boldsymbol{\theta}^*$. The three sets of optimal solutions are plotted in Figure 3, for the 23 tests conducted on the isolator prototypes. The optimal isolator model parameters obtained from the 23 data sets exhibit a large scatter, and this makes it difficult to choose a single set of the isolator parameters for the isolated bridge model. Thus the calibration of the isolator model needs to be performed using the recorded response of the bridge system to the 2010 Maule Earthquake. This need is further enhanced by a poor GOF of the bridge response to the 2010 Maule Earthquake when most of those parameter sets are used for the isolator elements of the bridge FE model, as found by the authors but not reported here for the space constraint.

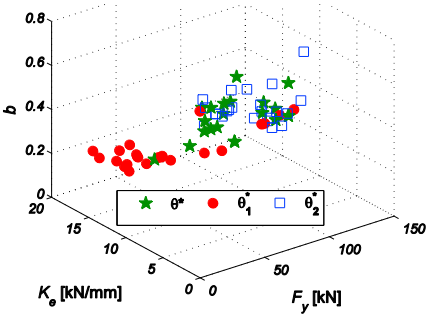

Fig. 3. Optimal isolator model parameter sets obtained from the component test data.

3.2. Estimation of isolator model parameters using field-recorded data during 2010 Maule, Chile Earthquake

A bridge system model with abutments excluded is employed to estimate the isolator model parameters (i.e., elastic stiffness K_e, yield strength F_y, and post-yield stiffness ratio b). The bridge displacement responses (obtained through double integration of the recorded acceleration responses) are used. Optimization problems considering single or multiple objective function(s) are formulated and solved using the grid-based brute-force approach by taking advantage of cloud-based high-throughput computing capabilities. The 3-D search domain for the isolator parameters is the same as that used for the isolator model calibration based on the component tests. This grid-based optimization task requires to run 1440 jobs of seismic response simulation of the bridge subjected to the 2010 Maule Earthquake with a long duration (i.e., 130 sec), which took less than 24 hours (wall-clock time) to complete all these jobs using high-throughput computing, approximately 800 times faster than running on a local desktop computer (Intel Core i7 CPU, 2.80 GHz, 8.0 GB RAM), when using the computational resources of the *Open Science Grid* (*OSG)* cluster at the University of California, San Diego, accessed via *GlideinWMS* [6].

Here, the RRMSEs for the prediction of the following response quantities are investigated: the absolute displacement response time history at the top of pier P#4 in the longitudinal and transverse directions, $U_{P\#4}^{Long.}$ and $U_{P\#4}^{Transv.}$; the absolute displacement response of the bridge deck over pier P#4 in the longitudinal and transverse directions, $U_{Deck\,over\,P\#4}^{Long.}$ and $U_{Deck\,over\,P\#4}^{Transv.}$; and the absolute displacement of the bridge deck over pier P#2 in the

transverse direction, $U^{Transv.}_{Deck\ over\ P\#2}$. These RRMSEs can be used for objective functions to be minimized in the FE model updating. Here, RRMES defined based on $U^{Long.}_{P\#4}$, $U^{Transv.}_{P\#4}$, and $U^{Transv.}_{Deck\ over\ P\#4}$, are used, denoted as F_1^{Obj}, F_2^{Obj}, F_3^{Obj}, respectively. Since the recorded horizontal motions at the bridge ends are imposed in the model and the longitudinal displacement of the bridge deck is negligibly affected by the seismic isolator properties, the RRMSE of $U^{Long.}_{Deck\ over\ P\#4}$ is insensitive to the variation of isolator model parameter, and thus not considered as an objection function. Additionally, the RRMSE of $U^{Transv.}_{Deck\ over\ P\#2}$ is not considered as an objective function as it changes similarly in the isolator parameter space to the RRMSE of $U^{Transv.}_{Deck\ over\ P\#4}$. A multi-objective optimization is also used to seek an overall good fit between FE-predicted and measured response for multiple response quantities from various channels. The square-root of a sum of squared single objective functions is used to indicate the overall GOF metric $\overline{RRMSE}$ as the weighted average of individual objective functions, denoted as F_R^{Obj}.

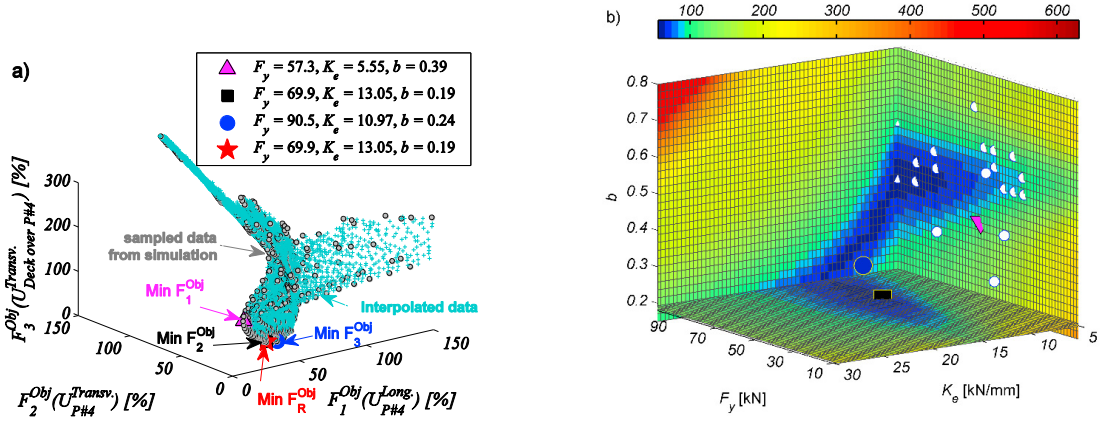

Fig. 4. (a) Optimization plots for nonlinear FEMU of the bridge, and (b) comparison of GOF metric $\overline{RRMSE}$ between isolator model parameter sets obtained from the component test data (i.e., white circles) and from recorded bridge response data.

Table 1. Optimum isolator model parameters obtained from single- and multi-objective FEMU formulations and corresponding GOF metrics.

Obj. fn.	Optimal isolator model parameters			RRMSE [%]				
	(kN)	(kN/mm)	(-)	$U^{Long.}_{P\#4}$	$U^{Transv.}_{P\#4}$	$U^{Transv.}_{Deck\ over\ P\#4}$	$U^{Long.}_{Deck\ over\ P\#4}$	$U^{Transv.}_{Deck\ over\ P\#2}$
F_1^{Obj}	57.3	5.55	0.39	20.42	15.84	96.43	6.13	82.78
F_2^{Obj}	69.9	13.05	0.19	35.10	13.16	42.12	6.27	47.47
F_3^{Obj}	90.5	10.97	0.24	43.73	13.88	36.68	6.24	45.73
F_R^{Obj}	69.9	13.05	0.19	35.10	13.16	42.12	6.27	47.47

Figure 4a shows the tri-objective optimization plot for nonlinear FEMU of the bridge with sampled data from FE response simulation and interpolation (of the individual GOF metrics inside the grid over the 3-D parameter space). The Pareto-optimal front in the 3-D parameter space can be observed as the cluster of points that are not dominated by any member of the parameter space. The minimum of each objective function (single-objective GOF metric), as well as the minimum of the weighted average objective function (multi-objective overall GOF metric), is marked in Figure 4a, and the corresponding RRMSE of the response quantities of interest are summarized in Table 1. When the overall GOF metric defined as F_R^{Obj}, the optimum solution obtained coincides with that for F_2^{Obj}. Therefore, the set of isolator model parameters that best fits the recorded response $U^{Transv.}_{P\#4}$ also yields accuracy in fitting the recorded responses $U^{Long.}_{P\#4}$ and $U^{Transv.}_{Deck\ over\ P\#4}$. It is observed that the best fit of the recorded response time history is achieved using the optimal set of isolator model parameters obtained from the single-objective optimization with the objective function defined based on the corresponding response quantity. Overall, when all the recorded response quantities in the longitudinal and transverse directions of the bridge are considered, the optimum sets of isolator model parameters obtained by minimizing F_R^{Obj}. Figure 4b compares the optimum sets of isolator model parameters obtained from component test data and from recorded bridge response data during the earthquake, and the corresponding GOF metric $\overline{RRMSE}$ (as color-coded) between the recorded and FE-predicted response time histories.

3.3. Reconstruction of seismic response

The bridge nonlinear FE model updated using a set of optimal isolator model parameters can now be used to reconstruct the unrecorded seismic response of the SIB during the earthquake. Here, the bridge FE model with the optimal set of isolator model parameters obtained using the multi-objective function F_R^{Obj}, is used to reconstruct the seismic response of the Marga-Marga Bridge to the 2010 Maule Earthquake. Figure 5 presents the moment-curvature response at the base of all seven pier-columns, and it is observed that the seven pier columns remain quasi elastic under this strong earthquake and the nonlinear behavior is concentrated in the seismic isolators.

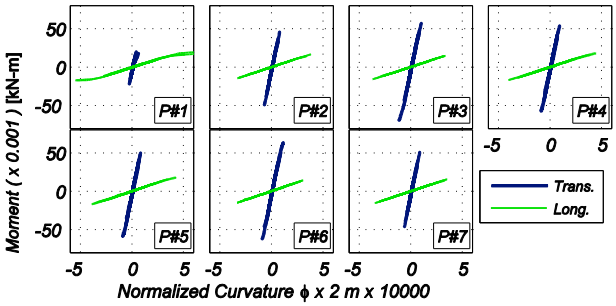

Fig. 5. Predicted unrecorded response quantities during the 2010 Maule Earthquake for moment-curvature response at the base of pier columns.

4. Conclusions

The seismic isolator model parameters are estimated using component test data and bridge response data during an earthquake. The isolator model parameters estimated from component tests show a large scatter, and a poor goodness-of-fit of the bridge response to the 2010 Maule Earthquake is obtained when most of those parameter sets are used for the isolator elements of the bridge FE model. However, the isolator model parameters estimated from the bridge response data recorded during the 2010 Maule Earthquake leads to good agreement between the FE-predicted and measured bridge response. The updated FE model can then be used to reconstruct unrecorded response quantities during the earthquake, in order to understand the effects of seismic isolation on the bridge response during a strong earthquake, and it is found that the bridge piers experienced little nonlinear behavior. This is claimed to be one of the benefits of nonlinear FE model updating, in contrast to the traditional linear FE model updating in which the updated model can rarely be used for the purpose of seismic response prediction.

Acknowledgements

Partial support of this research by (1) the Pacific Earthquake Engineering Research Center under Award No. 1107-NCTRCJ, and (2) the UCSD Academic Senate under Research Grant RN091G-CONTE is gratefully acknowledged. The authors thank Professor Maria O. Moroni and Professor Mauricio Sarrazin from the Department of Civil Engineering at the University of Chile for providing access to the data used in this study.

References

[1] M. Akiyama, D.M. Frangopol, Life-cycle design of bridges under multiple hazards Earthquake, tsunami and continuous deterioration. In Safety, Reliability, Risk, and Life-cycle Performance of Structures and Infrastructures, CRC Press. 2013.
[2] G. Housner, L. Bergman, T. Caughey, A. Chassiakos, R. Claus, S. Masri, R. Skelton, T. Soong, B. Spencer, J. Yao, Structural control: Past, present, and future. Journal of Engineering Mechanics ASCE, 123 (1997) 897–971.
[3] Y. Li, J.P. Conte, Effects of seismic isolation on the seismic response of a California high-speed rail prototype bridge with soil-structure and track-structure interactions. Earthquake Engineering & Structural Dynamics, 45(2016) 2415–2434.
[4] S. Mazzoni, F. McKenna, G.L. Fenves, OpenSees command language manual. http://opensees.berkeley.edu/. Pacific Earthquake Engineering Research. 2005.
[5] R. Boroschek, M. Moroni, M. Sarrazin, Dynamic characteristics of a long span seismic isolated bridge. Engineering Structures, 25(2003) 1479–1490.
[6] I. Sfiligoi, D. Bradley, H. Burt, M. Parag, P. Sanjay, W. Frank, The pilot way to grid resources using GlideinWMS. WRI World Congress on Computer Science and Information Engineering, Los Angeles, CA, 2009, pp. 428–432.